Inorganic Chemistry

Article

pubs.acs.org/IC

Water-Free Neodymium 2,6-Naphthalenedicarboxylates Coordination Complexes and Their Application as Catalysts for Isoprene Polymerization

Inês Rodrigues, Ionut Mihalcea, Christophe Volkringer, Thierry Loiseau,* and Marc Visseaux

Unité de Catalyse et Chimie du Solide (UCCS)—UMR CNRS 8181, Université de Lille Nord de France, USTL-ENSCL, Bat C7, BP 90108, 59652 Villeneuve d'Ascq, France

Supporting Information

ABSTRACT: A series of four coordination polymers based on neodymium have been hydrothermally synthesized with different carboxylic acids as a linker. The structures of the compounds $Nd_2(2,6\text{-ndc})_3(H_2O)_3{\cdot}H_2O$ (**1**), $Nd_2(2,6\text{-ndc})_2(ox)(H_2O)_2$ (**2**), and Nd(2,6-ndc)(form) (**3**) (2,6-ndc = 2,6-naphthalenedicarboxylate; ox = oxalate; and form = formate) have been determined by single-crystal X-ray diffraction analysis. They exhibit rather dense networks built up from infinite chains of NdO polyhedra connected to each other through the 2,6-ndc ligand. Terminal and bridging aquo species are present in the coordination sphere of Nd for **1**, whereas some of them are partially replaced by oxalate groups in **2** and fully substituted by formate groups in **3**. The water-free phase **3** as well as the compound $Nd(form)_3$ (**4**) were considered for catalytic reaction for polymerization of isoprene in the presence of Al-based cocatalyst, affording *cis*-polyisoprene with good conversions. Residual Nd material with unchanged structure was found in the polymeric material. The neodymium luminescence of compounds **3** and **4** was also measured.

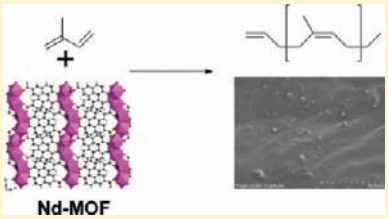

INTRODUCTION

The interest for the new class of porous coordination polymers (PCPs) or metal−organic frameworks (MOFs) has grown exponentially for the past decade, and many potential applications have been discovered in the area of molecular storage and separation, drug delivery, etc.[1−6] These crystalline materials have attracted special attention since their well-defined atomic architectures delimit large cavities or channels systems (micro- and mesoscale), which are generated by the three-dimensional connection of metallic nodes through organic N- or O-donor ligands. Aromatic molecules are usually employed to form rigid extended networks, which remain stable enough upon the removal of solvent species trapped within the pores. The association of metallic cores together with organic linkers gives rise to a wide variety of arrangements, due to the richness of organic chemistry for the elaboration of functionalized molecules and also the diversity of metal candidates from the periodic table. In this context, the choice of metal will be governed by following the chemical or physical targeted properties. This aspect is especially a key point in the field of catalysis, for which the nature of metallic cations is known to play a significant role for enhancing a chemical reaction. In this domain, the porous networks of PCP or MOF solids have been recently considered as heterogeneous catalysts, which combine the occurrence of active metal sites together with confined nanoreactors related to the shape and size of the structure pores. Several reviews have reported these emerging catalysis applications in MOF type materials.[7−11] One of this field concerns the synthetic polyisoprene, which is found in the rubber and tires industry. A family of very efficient coordination catalysts for this purpose is based on the rare earths, particularly neodymium,[12−15] and continuous effort is made to improve catalytic systems with the aim to get better activity and higher selectivities. Lanthanide carboxylates, associated with aluminum cocatalysts, have been widely used in the industry in this frame since the last two decades after the pioneering investigation in the early 1970s.[16] It was shown only recently that neodymium-based carboxylate MOF type materials can be efficiently used for polymerization of isoprene.[17] We therefore are continuing to investigate the study of the reactivity of such compounds as potential Ziegler−Natta catalysts in conjugated diene polymerization. One prerequisite is the absence of any aquo or hydroxo ligands bonded to the metal in the coordination polymer, which makes the catalytic reaction unproductive. This consideration would limit the number of potential solids since they should be stable enough upon dehydration or dehydroxylation processes or do not contain any of these species. The aspect could be critical since most of the lanthanide-based MOF compounds have aquo ligands within their coordination sphere and synthesis strategies must be oriented to avoid such ancillary OH_n coordinating ligands. One solution could be the use of nonaqueous solvent (*N*,*N*-dimethylformamide, methanol, etc.) for the crystallization, but solvent molecules usually belong to the metal environment in the final crystalline solid.

In this contribution, we propose an alternative approach with the association of two types of ligands, with different steric hindrances. We selected the 2,6-naphthalenedicarboxylate (noted 2,6-ndc), a linear rigid ditopic linker that we combine with oxalate (noted ox) or formate (noted form) species. This

Received: September 2, 2011
Published: December 14, 2011

   dx.doi.org/10.1021/ic2019346 | *Inorg. Chem.* 2012, 51, 483−490

naphthalene-based ligand has been previously used for the formation of various porous compounds such as the isoreticular solids IRMOF-8[18] or MOF-69[19] or solids based on trivalent *p* (Al[20,21]) or *f* elements (rare earths[22]). With the lanthanide cations, different coordination polymers already have been reported, for which ancillary solvent water[23−28] or *N*,*N*-dimethylformamide[29] species are present in the surrounding cations. In our study, the oxalate or formate linkers were used as a substituent of aquo ligands to generate carboxylate network with oxo bridges only. The combination of oxalate or formate ligands with other carboxylate linkers has been previously described in the literature.[30−40]

The present work deals with the description of the different phases obtained from the chemical system Nd/2,6-ndc/H_2O in mild hydrothermal conditions (autogenous pressure) and examines the structural effect of the addition of oxalate or formate species in the reaction medium. Three coordination polymers thus have been isolated $Nd_2(2,6\text{-ndc})_3(H_2O)_3{\cdot}H_2O$ (**1**), $Nd_2(2,6\text{-ndc})_2(ox)(H_2O)_2$ (**2**), and Nd(2,6-ndc)(form) (**3**). Only the mixed formate-naphthalenedicarboxylate phase has no coordinated water. During our investigations, a fourth phase, consisting of an anhydrous neodymium formate network,[41] $Nd(form)_3$ (**4**), also has been prepared. The crystal structures of the compounds **1**, **2**, and **3** have been analyzed by means of single-crystal X-ray diffraction. The water-free compounds **3** and **4** have been further considered as precatalysts for the polymerization of isoprene in the presence of methylaluminoxane (MAO) or modified methylaluminoxane (MMAO). Both compounds were found efficient, with mixed ligand complex **3** giving rise to a more *cis*-selective catalyst, up to 88%.

EXPERIMENTAL SECTION

Materials. Neodymium chloride hexahydrate ($NdCl_3{\cdot}6H_2O$, Aldrich, 99.9%), 2,6-naphthalenedicarboxylic acid ($HO_2C{-}C_{10}H_6{-}CO_2H$, noted 2,6-$H_2$ndc, Aldrich, 99%), oxalic acid dihydrate ($C_2O_4H_2{\cdot}2H_2O$, noted $H_2ox{\cdot}2H_2O$, Aldrich, 99%), formic acid (HCO_2H, noted Hform, Aldrich, ≥95%), potassium hydroxide (KOH, Prolabo), ammonium hydroxide (Prolabo, 28%), *N*,*N*-dimethylformamide (Aldrich, ≥99.8%), and deionized water have been used without any further purification. MAO (Aldrich, toluene solution, 10% Al, 1.48 M), MMAO (Akzo Nobel, heptane solution, 7% Al, 18% MMAO, 1.84 M), Al(i-Bu)$_3$ (Aldrich, 99%), and $AlEt_2Cl$ (Aldrich, 1.8 M toluene solution) were used as received. Isoprene (Aldrich, 99.9%) was distilled twice over CaH_2 and molecular sieves (3 A) and then stored at −20 °C in a glovebox. Toluene was purified through alumina column (Mbraun SPS).

Synthesis. The compounds have been hydrothermally synthesized under autogenous pressure using Teflon-lined Parr type autoclaves.

*$Nd_2(2,6\text{-ndc})_3(H_2O)_3{\cdot}H_2O$ (**1**).* A mixture of 0.359 g (1 mmol) of $NdCl_3{\cdot}6H_2O$, 0.109 g (0.5 mmol) of 2,6-naphthalenedicarboxylic acid, 0.6 mL (0.6 mmol) of 1 M KOH, and 4.4 mL (240 mmol) of H_2O was placed in a Parr bomb and then heated statically at 180 °C for 24 h. The solution pH was 2.4 at the end of the reaction. The resulting pink product was then filtered off, washed with water, and dried at room temperature. After the hydrothermal reaction, a mixture of **1** and unreacted 2,6-H_2ndc crystallites was obtained. The latter could be easily removed by further washing with *N*,*N*-dimethylformamide. Elemental analysis, observed (calculated): C, 46.2% (43.1%); H, 2.5% (2.6%).

*$Nd_2(2,6\text{-ndc})_2(ox)(H_2O)_2$ (**2**).* A mixture of 0.360 g (1 mmol) of $NdCl_3{\cdot}6H_2O$, 0.055 g (0.25 mmol) of 2,6-naphthalenedicarboxylic acid, 0.032 g (0.25 mmol) of oxalic acid dihydrate, 1.5 mL (3 mmol) of 2 M NH_3 in water, and 3.5 mL (194 mmol) of H_2O was placed in a Parr bomb and then heated statically at 180 °C for 24 h. The solution pH was 4.8 at the end of the reaction. The resulting pink product was then filtered off, washed with water, and dried at room temperature. After the hydrothermal treatment, a mixture of compounds **1** and **2** was obtained.

*Nd(2,6-ndc)(form) (**3**).* A mixture of 0.180 g (0.5 mmol) of $NdCl_3{\cdot}6H_2O$, 0.032 g (0.9 mmol) of 2,6-naphthalenedicarboxylic acid, 0.5 mL (13 mmol) of formic acid, 1.8 mL (23 mmol) of *N*,*N*-dimethylformamide, and 2.2 mL (120 mmol) of H_2O was placed in a Parr bomb and then heated statically at 180 °C for 24 h. The resulting yellow product was then filtered off, washed with water, and dried at room temperature. Elemental analysis, observed (calculated): C, 35.7% (35.8%); H, 1.0% (1.6%).

*$Nd(form)_3$ (**4**).* The preparation of **4** was recently described in literature.[42] We used a closely related protocol for its synthesis: A mixture of 0.360 g (1 mmol) of $NdCl_3{\cdot}6H_2O$, 3 mL (79 mmol) of formic acid, and 2 mL (2 mmol) of 1 M KOH was placed in a Parr bomb and then heated statically at 180 °C for 24 h. The solution pH was 1.45 at the end of the reaction. The resulting pink product was then filtered off, washed with water, and dried at room temperature. Elemental analysis, observed (calculated): C, 12.6% (12.9%); H, 0.2% (1.1%).

Single-Crystal X-ray Diffraction. Crystals were selected under polarizing optical microscope and glued on a glass fiber for a single-crystal X-ray diffraction experiment. X-ray intensity data were collected on a Bruker X8-APEX2 CCD area detector diffractometer using Mo Kα radiation (λ = 0.71073 Å) with an optical fiber as collimator. Several sets of narrow data frames (20 s per frame) were collected at different values of θ for 2 and 2 initial values of ϕ and ω, respectively, using 0.3° increments of ϕ or ω. Data reduction was accomplished using SAINT V7.53a.[43] The substantial redundancy in data allowed a semiempirical absorption correction (SADABS V2.10[44]) to be applied, on the basis of multiple measurements of equivalent reflections. The structure was solved by direct methods, developed by successive difference Fourier syntheses, and refined by full-matrix least-squares on all F^2 data using SHELX[45] program suite with the WINGX[46] interface. Hydrogen atoms of the benzene ring were included in calculated positions and allowed to ride on their parent atoms. The final refinements include anisotropic thermal parameters of all nonhydrogen atoms and were performed using the SHELX program on the basis of F^2. The crystal data are given in Table 1. The Supporting Information is available in CIF format.

Isoprene Polymerization. All preliminary operations were carried out in a glovebox (Jacomex). In a typical polymerization, a flask was charged with the MOF precatalyst. The solvent (toluene, 1 mL) and the cocatalyst (MAO or MMAO) were added with syringes. In all attempts, the mixture was magnetically stirred for 20 min at room temperature before adding the monomer (isoprene, 0.68 g, 1 mL, 10 mmol). The polymerization was conducted outside the glovebox, under an inert atmosphere, at a given monitored temperature and running time. The viscous mixture was quenched with methanol containing 2,6-di-*tert*-butyl-4-methylphenol (1.0 wt %) as a stabilizer. The resulting isolated polymeric material was dried under vacuum at room temperature to a constant weight. The yield was determined by gravimetry.

Polymer Characterization. The selectivity was determined by ^{1}H NMR and ^{13}C NMR according to published methods.[47] The NMR spectra were recorded on an AC 300 Bruker at 300 MHz, in chloroform-D solutions. Approximately 5 and 40 mg of sample were directly dissolved into the NMR tube in 0.6 mL of solvent for ^{1}H and ^{13}C NMR, respectively. The chemical shifts were calibrated using the residual resonances of the solvent. Quantitative ^{13}C NMR was realized using the *zgig* sequence (Bruker library). The relaxation time d1 was set to 2, 5, and 8 s, and it was found that a relaxation time of 5 s is necessary to allow the relaxation of all carbon nuclei. Size-exclusion chromatography (SEC) was performed in tetrahydrofuran (THF) as an eluent at 20 °C using a Waters 410 refractometer and a Waters Styragel column (HR2, HR3, HR4, and HR5E) calibrated with polystyrene standards.

Luminescence Spectroscopy. Raman spectra were recorded on a FT-Raman Bruker spectrometer, model RSF 100, at room temperature. The excitation source was a YAG:Nd laser ($\lambda_{Exc.}$ =

dx.doi.org/10.1021/ic2019346 | *Inorg. Chem.* 2012, 51, 483−490

Table 1. Crystal Data and Structure Refinement for Different Neodymium 2,6-Napthalenedicarboxylates

	1	2	3
formula	$C_{18}H_9NdO_8$	$C_{13}H_6NdO_7$	$C_{13}H_7NdO_6$
formula weight	497.49	418.42	403.43
temperature (K)	293(2)	293(2)	293(2)
crystal type	pink	pink	pink
crystal size (mm^3)	0.51 × 0.43 × 0.11	0.46 × 0.08 × 0.04	0.18 × 0.16 × 0.09
crystal system	monoclinic	orthorhombic	monoclinic
space group	$P2_1/n$	$Pbca$	$P2_1/c$
a (Å)	17.1900(3)	10.7908(11)	13.0575(9)
b (Å)	15.1901(3)	8.6951(9)	13.0531(9)
c (Å)	25.3382(5)	25.475(2)	6.9251(4)
α (°)	90	90	90
β (°)	106.581(1)	90	94.070(3)
γ (°)	90	90	90
volume (Å^3)	6341.1(2)	2390.3(4)	1177.34(1)
Z, ρ_{calcd}(g cm^{-3})	16, 2.084	8, 2.325	4, 2.276
μ (mm^{-1})	3.324	4.378	4.433
Θ range (°)	1.28−37.62	1.60−30.78	1.56−33.78
limiting indices	$-29 \le h \le 29$	$-15 \le h \le 15$	$-20 \le h \le 20$
	$-26 \le k \le 25$	$-9 \le k \le 12$	$-20 \le k \le 20$
	$-43 \le l \le 41$	$-36 \le l \le 34$	$-10 \le l \le 10$
collected reflections	194453	45287	73399
unique reflections	33503	3738	4714
	[R(int) = 0.0423]	[R(int) = 0.0557]	[R(int) = 0.0562]
parameters	974	191	181
goodness-of-fit on F^2	1.103	1.362	1.172
final R indices [$I > 2\sigma(I)$]	$R1$ = 0.0358	$R1$ = 0.0308	$R1$ = 0.0246
	$wR2$ = 0.0902	$wR2$ = 0.0690	$wR2$ = 0.0614
R indices (all data)	$R1$ = 0.0588	$R1$ = 0.0492	$R1$ = 0.0388
	$wR2$ = 0.1105	$wR2$ = 0.0981	$wR2$ = 0.0832
largest diff. peak and hole (e Å^{-3})	5.746 and −1.367	1.891 and −0.960	1.066 and −1.258

1064 nm) (excitation power 100 mW and an optical aperture of 1.1). The energy values from Raman shift (cm^{-1}), E_R, were converted into emission energy (cm^{-1}), E_E, using the expression: $E_E = E_{laser} - E_R$, where E_{laser} = 9398.5 cm^{-1}. Subsequently, the E_E values were converted in wavelengths (nm).

RESULTS

Structure Descriptions. *Crystal Structure of $Nd_2(2,6\text{-}ndc)_3(H_2O)_3{\cdot}H_2O$ (1).* Compound **1** has a parent structure with other hydrated rare-earth naphthalenedicarboxylates containing Pr,[25] Eu,[25] Tb,[48] and Ho,[26] crystallizing in a similar monoclinic cell ($P2_1/n$, $a \approx 17.0$, $b \approx 15.1$, $c \approx 25.0$ Å, $\beta \approx 106.4°$). Its structure is built up from four crystallographically independent neodymium centers in 9-fold coordination (Figure 1). Each inorganic cation is surrounded by six carboxyl oxygen atoms with Nd−O distances ranging from 2.367(2) up to 2.533(2) Å. Longer Nd−O bonds [2.863(2)−2.906(2) Å] also occur and correspond to a μ_3 connection mode for one carboxyl oxygen atom, which bridges two adjacent neodymium cations and one carbon atom from a carboxylate arm of the organic linker. Water species are found in terminal position with Nd−Ow distances of 2.495(2)−2.595(2) Å range (O27, O29, O25, and O30; Ow stands for water oxygen) and in bridging fashion [Nd−Ow = 2.699(2)−2.830(2) Å; O20 and O28] between two neighboring neodymium cations. The assignment to such μ_2- or η_1-aquo groups is in good agreement with the bond valence

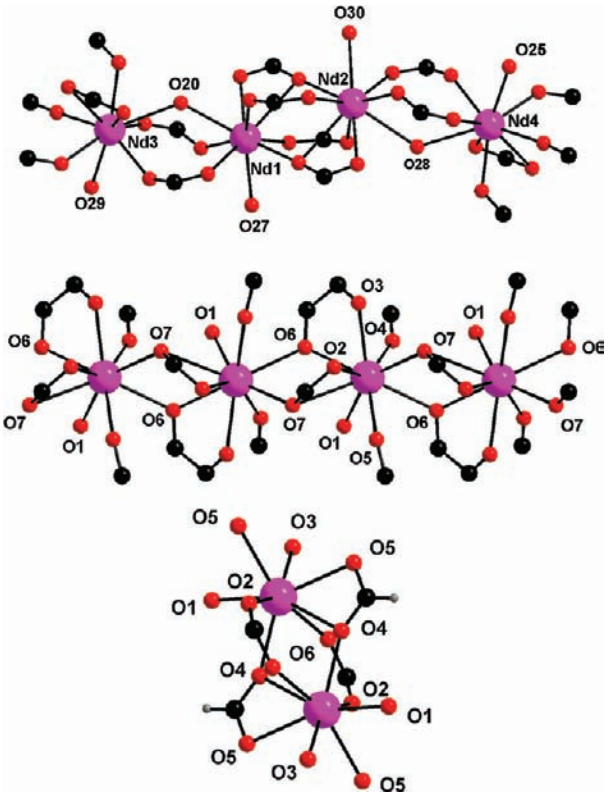

Figure 1. Details of the coordination environments of the four independent neodymium cations forming infinite ribbons in $Nd_2(2,6\text{-}ndc)_3(H_2O)_3{\cdot}H_2O$ (**1**). O25, O27, O29, and O30 correspond to terminal water species, whereas O20 and O28 are μ_2-bridging water species. Only carbon atoms of the carboxylate groups are shown for clarity (top). Details of the 9-fold coordinated neodymium environments forming infinite ribbons in $Nd_2(2,6\text{-ndc})_2(ox)(H_2O)_2$ (**2**). O1 corresponds to terminal water molecule. O6 and O7 belong to oxalate and naphthalenedicarboxylate, respectively, and are μ_3-oxo bridges between two neighboring neodymium centers (middle). View of the dinuclear unit containing 2-fold-coordinated neodymium centers in Nd(2,6-ndc)(form) (**3**) (bottom).

calculations[49] (0.33−0.38 and 0.27−0.36, respectively). The resulting environment (6 μ_2-Oc + 1 μ_3-Oc + η_1-H_2O + μ_2-H_2O; Oc stands for carboxyl oxygen) for neodymium gives rise to the formation of infinite chains of distorted monocapped antiprism polyhedra $NdO_7(H_2O)_2$, running along the a-axis. Within the inorganic ribbons, pairs of edge-sharing neodymium-centered polyhedra [Nd1···Nd2 = 4.112(1) Å and Nd3···Nd4 = 4.114(1) Å] strictly alternate with corner-sharing ones (Nd1···Nd3 and Nd2···Nd4). The chains are linked to each other via the carboxylate arms of the six crystallographically independent naphthalenedicarboxylate ligands, which adopt either a μ_4-$\eta_1{:}\eta_1{:}\eta_1{:}\eta_1$ (each carboxylate group is *syn*−*syn* bidentate) or μ_5-$\eta_2{:}\eta_1{:}\eta_1{:}\eta_1$ connection mode. For the latter, the carboxylate groups are either *syn*−*syn* bidentate or both asymmetric chelating and *syn*−*anti* bidentate. It results in the formation of three-dimensional neutral framework delimiting closely packed channels developing along the a-axis, parallel to the direction of the inorganic chains (Figure 2). Within the tunnels are located two independent water molecules in strong hydrogen bond interactions to each other [2.859(9) Å] and also with the terminal water molecules O29 attached to Nd3 [2.997(6) Å] and O30 attached to Nd2 [2.869(8) Å]. This topological feature is reminiscent of that occurring in the

dx.doi.org/10.1021/ic2019346 | Inorg. Chem. 2012, 51, 483−490

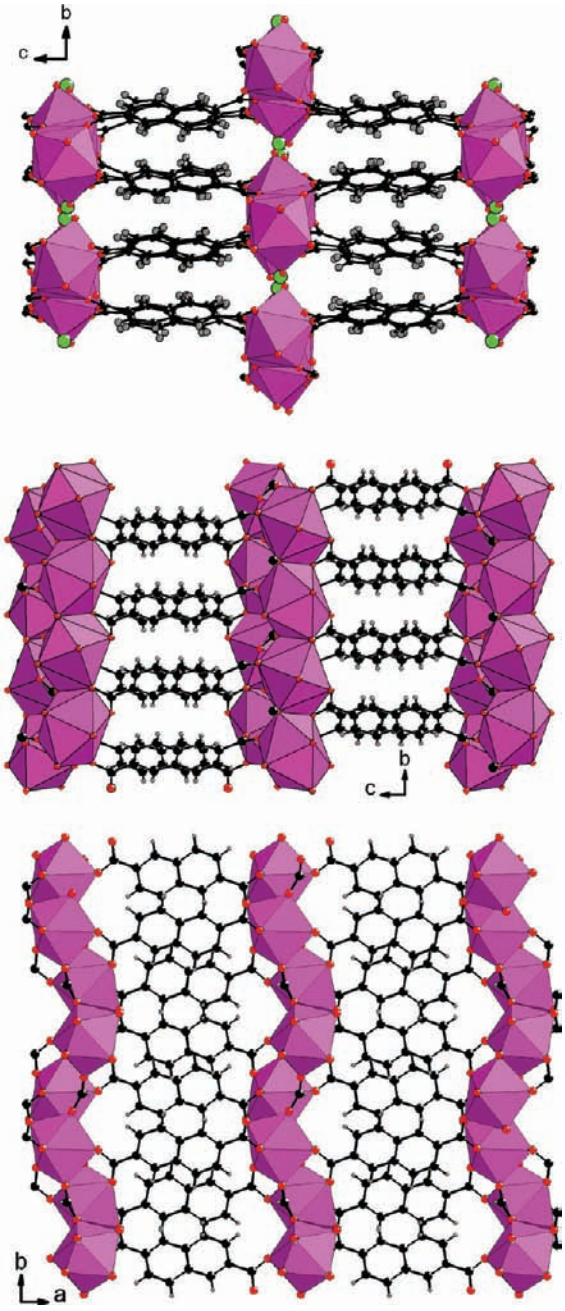

Figure 2. View of the 3D structure of $Nd_2(2,6\text{-ndc})_3(H_2O)_3{\cdot}H_2O$ (**1**) along the *a*-axis, showing the free water species (green circles) encapsulated within channels (top). View of the 3D structure of **2** along the *a*-axis, showing the connection of mixed organic−inorganic layer $Nd_2(2,6\text{-ndc})_2(ox)(H_2O)_2$ through the 2,6-ndc ligand (middle). View of the 3D structure of **3** along the *c*-axis, showing the connection of the mixed organic−inorganic layer Nd(2,6-ndc)(form) through the 2,6-ndc ligand (bottom).

trivalent aluminum naphthalenedicarboxylate (MIL-69[20,21]), which also possesses a lozenge-shape channels like network based on the chains of octahedral units intercrossing with the organic spacer. Other variants of this structure type are reported with different rare earths and concern the content of water bonded to the cations (Ho,[26] Yb[24]). X-ray thermodiffraction experiment (see the Supporting Information) indicates that Bragg peaks are clearly visible up to 180 °C, which then persist up to 440 °C but with lower intensities. Above this

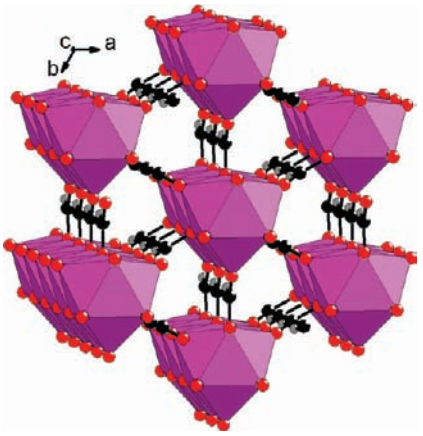

Figure 3. Perspective view of the structure of $Nd(form)_3$ (**4**) along the *c*-axis, showing the connection of the isolated neodymium-centered tricapped trigonal prisms NdO_9 via the formate ligands.

temperature, the decomposed phase is transformed into the cubic form Nd_2O_3 (500−740 °C), and then, the hexagonal form Nd_2O_3 appears.[50]

*Crystal Structure of $Nd_2(2,6\text{-ndc})_2(ox)(H_2O)_2$ (**2**).* The compound **2** still displays a hydrated network but with a lower content as compared to that of **1**. Its structure consists of one crystallographically independent 9-fold coordination defining a distorted monocapped square antiprism. It is surrounded by eight carboxyl oxygen atoms (Figure 1). Four of them (O2, O3, O4, and O5) have a μ_2 connection fashion with Nd−O distances in the range 2.419(4)−2.496(3) Å. Four (2 × O6 and 2 × O7) of them a μ_3 connection fashion with longer Nd−O bonds [2.608(3) and 2.792(4) Å] since they are involved in a bridging mode between two neighboring rare-earth cations and a carboxylate group of the organic part (either ox or 2,6-ndc). The remaining nonbonded oxygen (O1) is a terminal water molecule with Nd−O distance of 2.459(4) Å, in good agreement with bond valence[49] calculations (0.40). Because of the occurrence of μ_3-oxo groups, chains of edge-sharing neodymium centered monocapped square antiprismatic polyhedra $NdO_8(H_2O)$ are generated along the *b*-axis, with Nd···Nd distance of 4.349(1) Å. The oxalate group is connected to four neodymium cations as a hexadentate bridging linker between two adjacent inorganic ribbons, with the μ_4-η_2:η_1:η_2:η_1 configuration. The naphthalenedicarboxylate molecules also contribute as bridging linker between two chains through one of its carboxylate arm (*syn*−*syn* bidentate connection mode). The remaining carboxylate group acts as both an asymmetric chelating and a bidentate (*syn*−*anti*) bridging linker with neodymium centers of a given inorganic chain. The connection mode is μ_4-η_2:η_1:η_1:η_1. It results in the formation of a neutral mixed organic−inorganic layer $Nd_2(2,6\text{-ndc})_2(ox)(H_2O)_2$ developing in the (*a*,*b*) plane. The naphthalenedicarboxylate linker perpendicularly connects the hybrid sheets along the *c*-axis to form a rather compact three-dimensional edifice without any void (Figure 2).

*Crystal Structure of Nd(2,6-ndc)(form) (**3**).* When replacing the oxalate linker by the formate ones, an anhydrous phase (**3**) is revealed from X-ray diffraction analysis. Its structure is built up from one crystallographically independent neodymium center with an 8-fold coordination, which differs from the previous hydrated compounds, which have terminal η_1-aquo ligands and, therefore, a higher coordination state. The geometric polyhedron surrounding the rare-earth atom is a

dx.doi.org/10.1021/ic2019346 | *Inorg. Chem.* 2012, 51, 483−490

Table 2. Isoprene Polymerization with Nd(2,6-ndc)(form) (3) and Nd(form)$_3$ (4) as Precatalysts

run[a]	precatalyst	cocatalyst	T (°C)	time (h)	yield (%)	Mn_{exp} (PDI)[b]	Mn_{th}[c]	selectivity (%)[d] *cis-/trans-*/3,4- (%)
1	**4**	100 MMAO	50	96	33.4	38000 (3.40)	12600	80.5/6.9/12.6
2	**4**	100 MMAO	80	24	29.0	148000/10900 (multimodal)	11000	69.0/17.6/13.4
3	**4**	100 MMAO	80	96	54.5	61000/5700 (bimodal)	20600	57.2/26.6/16.2
4	**4**	300 MMAO	80	24	27.0	39600/5600 (bimodal)	10200	71.8/13.8/14.4
5	**4**	100 MAO	50	24	28.8	15300 (2.84)	10900	61.7/29.0/9.3
6	**4**	50 MAO	80	96	83.6	24100 (2.55)	31600	48.0/40.3/11.7
7	**4**	100 MAO	80	96	77.0	20000 (2.69)	29100	53.6/37.0/9.2
8	**4**	300 MAO	80	96	76.5	5700 (3.68)	28900	55.2/30.4/14.4
9	**4**	10 $AliBu_3$/2 $AlEt_2Cl$	80	24	0			
10	**3**	100 MMAO	50	24	32.2	139000 (1.80)	10900	84.5/7.7/7.8
11	**3**	100 MMAO	50	72	48.2	69000 (4.15)	16400	88.7/4.9/6.4
12	**3**[e]	100 MMAO	50	24	64.3	172000/17000 (bimodal)	21900	83.5/7.9/8.6

[a] $V_{toluene} = V_{isoprene}$ = 1 mL; precatalyst **4**: 18 μmol, [isoprene]/[Nd] = 556; precatalyst **3**: 20 μmol, [isoprene]/[Nd] = 500. [b] Determined by SEC with reference to polystyrene standards; PDI = M_w/M_n. [c] Calculated from yield × [isoprene]/[Nd] × 68 (one polymer chain per Nd). [d] From ^{1}H and ^{13}C NMR. [e] The solid was ground in a mortar for 10 min and subsequently dried in an oven at 100 °C overnight.

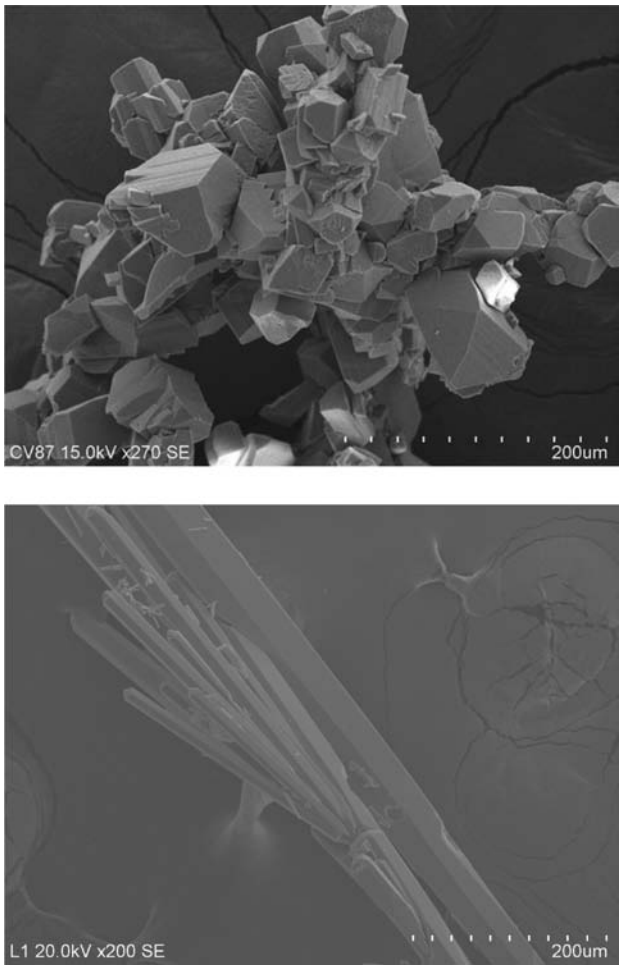

Figure 4. SEM images of Nd(2,6-ndc)(form) (**3**, top) and Nd(form)$_3$ (**4**, bottom).

distorted square antiprism NdO_8, with Nd−O distances ranging from 2.330(2) up to 2.654(2) Å, which can be divided into two groups. Four of the oxygen atoms (O1, O2, O3, and O6) belong to carboxylate groups of the 2,6-ndc linker with Nd−O distances of 2.330(2)−2.400(2) Å range. The four others (O4 and O5) coordinate two neighboring neodymium atoms and also belong to formate groups. Longer Nd−O bondings [2.443(2)−2.654(2) Å] reflect this μ_3-connection fashion. Two of this μ_3-oxo groups bridge two neodymium via a common corner whereas the two others bridge the inorganic cations via a common edge, resulting in a dinuclear motif with a relatively short Nd···Nd distance of 4.0564(3) Å (Figure 1). The formate anions are thus linked to two neodymium atoms in both symmetric chelating and *syn−anti* bidentate bridging modes (μ_2-η_2:η_1). The carboxylate arms of the naphthalenedicarboxylate groups bridge two inorganic cations through a *syn−syn* and *syn−anti* bidentate fashion (μ_4-η_1:η_1:η_1:η_1). This generates a neutral two-dimensional network with the pavement of the connection of dinuclear building blocks adopting two orientations in the (*b*,*c*) plane. It represents a distorted hexagonal net with the Schläfli symbol 6^3 if one considers the neodymium centers as nodes. In this organic−inorganic sheet, the hydrogen atoms of formate are pointing toward the center of the hexagonal ring of the 6^3 net, parallel to the (*b*,*c*) plane, whereas the carboxylate groups of the 2,6-ndc are pointing upward and downward the layer in the [100] direction. The three-dimensional cohesion of the structure is ensured by the ditopic 2,6-ndc ligands, which connect the organic−inorganic sheets to each other, along the *a*-axis (Figure 2). It is also noted that coordination polymers involving both carboxylate and formate linkers are rarely described in literature. Only a few examples reported such structural feature,[37−40] for which formate ligands are generated in situ during the hydrothermal reaction from the decomposition of an organic solvent such as *N*,*N*-dimethylformamide. X-ray thermodiffraction experiment (see the Supporting Information) shows that the phase is stable up to 420 °C, and it is then decomposed and recrystallizes into the cubic form Nd_2O_3 (540−680 °C) followed by the transformation into the hexagonal phase Nd_2O_3.[50]

Crystal Structure of Nd(form)$_3$ (4). Its three-dimensional structure type was previously reported by many authors with different trivalent lanthanide cations (La, Ce, Pr, Nd, Sm, Gd, Tb, Ho, Er, and Tm).[41,42,51−56] The structure of the neodymium formate was recently redetermined from single-crystal analysis in a rhombohedral symmetry.[41,42] It is based on the connection of infinite ribbons of tricapped trigonal prismatic polyhedra NdO_9, linked to each other via the formate groups, which adopt the bidentate bridging mode μ_3-η_2:η_1 (Figure 3). The linkage of the NdO_9 polyhedra occurs through trigonal faces with three μ_3-oxo species. X-ray thermodiffraction

dx.doi.org/10.1021/ic2019346 | *Inorg. Chem.* 2012, 51, 483−490

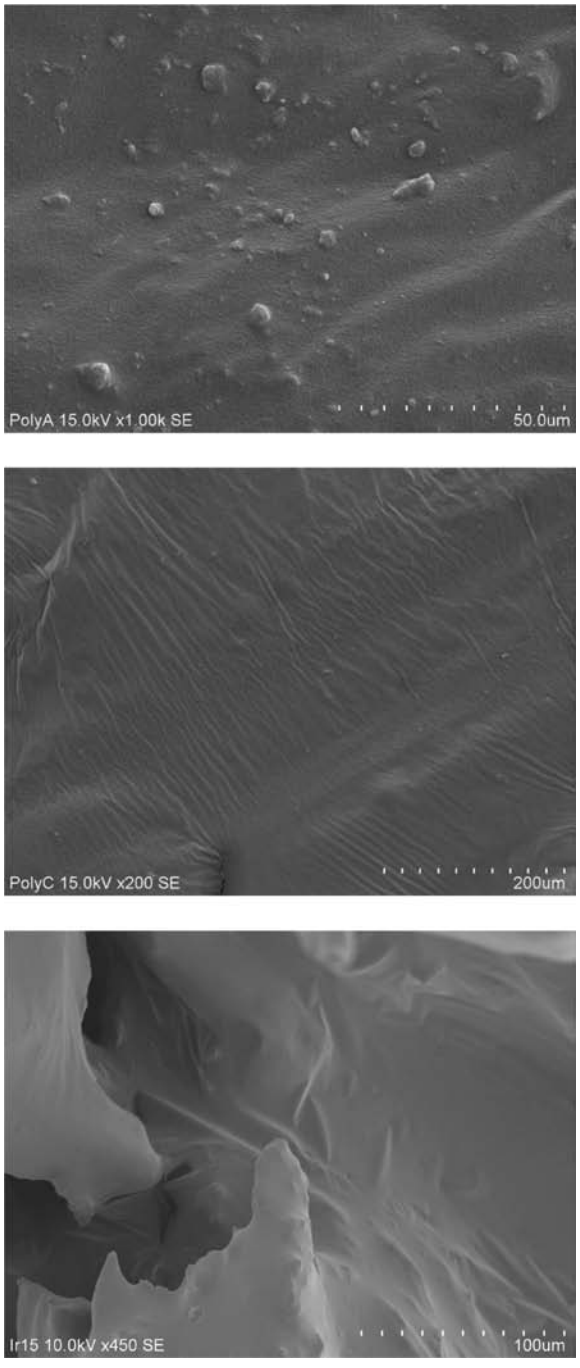

Figure 5. SEM images of the polyisoprene surface produced with Nd(2,6-ndc)(form) (**3**), which was used under two different forms: as-synthesized crystalline powder (top) and manually grinded powder (middle). SEM image of the polyisoprene surface produced with $Nd(form)_3$ (**4**) (bottom).

experiment (see the Supporting Information) indicate that this phase is stable up to 300 °C and then transformed into $Nd_2O_2CO_3$ (pdf file 25-0567) between 380 and 640 °C. Above this temperature, a mixture of the cubic and hexagonal is observed.[50]

Production of Polyisoprene. *Polymerization Catalysis.* As water-free, homoleptic $Nd(form)_3$ (**4**) and mixed ligand Nd(2,6-ndc)(form) (**3**) compounds were assessed as precatalysts toward isoprene polymerization. Because they are built from neodymium carboxylate, the polymerization activity could

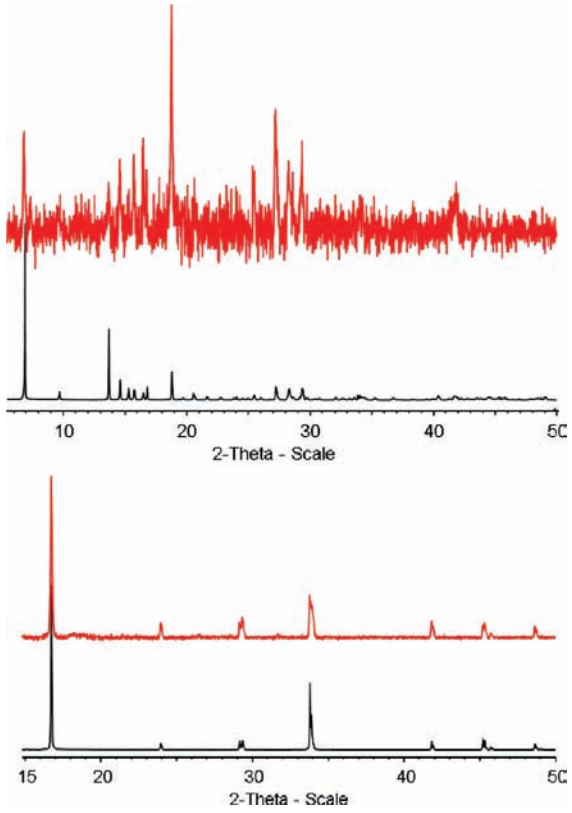

Figure 6. Comparison of XRD patterns of Nd(2,6-ndc)(form) (**3**, top) and $Nd(form)_3$ (**4**, bottom) as synthesized (black) and dispersed in isoprene (red).

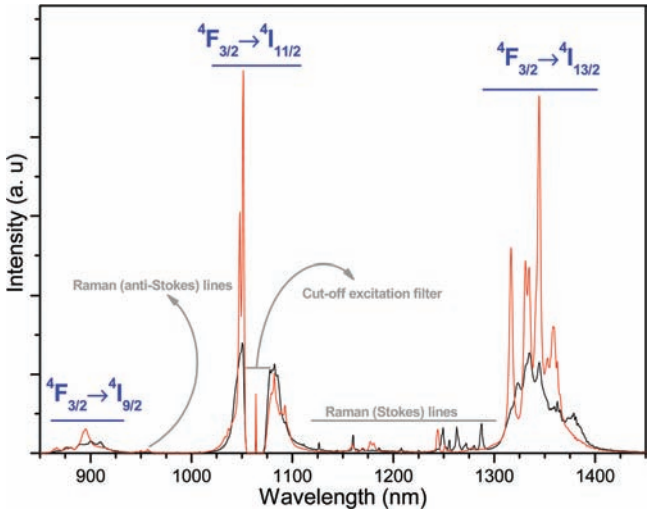

Figure 7. FT-Raman spectra of Nd(2,6-ndc)(form) (**3**, black line) and $Nd(form)_3$ (**4**, red line) samples recorded at room temperature. The excitation source was a YAG:Nd laser ($\lambda_{Exc.}$ = 1064 nm) with an excitation power of 100 mW.

be expected so far as several reports based on related complexes have been published since the last two decades.[13,16] We found that both coordination compounds are efficient when combined with aluminoxanes cocatalysts; selected results are gathered in Table 2. However, as already observed for other neodymium carboxylate-based MOFs, heating (at least 50 °C) and long reaction times (>20 h) are necessary to isolate some

dx.doi.org/10.1021/ic2019346 | *Inorg. Chem.* 2012, 51, 483−490

polymer material. This moderate reactivity is probably related to the heterogeneous nature of the catalytic system.[17]

Experiments were first carried out with **4** combined to MMAO and MAO. It is noteworthy that the latter cocatalyst gives higher conversions (ca. 70−80% at 80 °C, runs 6−8), whereas the selectivity is better with MMAO: polyisoprene 81% *cis*-regular was obtained at low temperature (run 1) with **4**/MMAO and nearly 72% *cis* with larger amounts of cocatalyst (run 4) as already reported with MIL-n compounds. These results prompted us to study the behavior of compound **3** in the same conditions. Associated to MMAO, coordination compound **3** was found more active than **4**, since satisfactory polymer yield is obtained at only 50 °C (64% in 28 h, run 12). Moreover, much higher *cis*-selectivity is reached (88.7% *cis*-regular, run 12). Raising the temperature from 50 to 80 °C causes higher conversion but is detrimental to the selectivity of the process. As a comparison, the polymer yield with MIL-103,[17] for comparable *cis*-selectivities (ca. 90%), never exceeded 30% polymer yield at 50 °C. The impact of grinding of the MOF precatalyst toward the catalytic performances was also assessed. We observed a positive effect in terms of polymer productivity (64 vs 32%, runs 12 vs 10, respectively), while keeping high *cis*-selectivity. Surprisingly, replacing the aluminoxane by $Al(i\text{-}Bu)_3/AlEt_2Cl$, as alternatively proposed for Nd carboxylate-based polymerizations,[16] was ineffective in our case (run 9).

Regarding macromolecular data, when activated with MMAO, precatalysts **3** (runs 10−12) and **4** (runs 1−4) give polymer with broad molecular weight distribution, all having a bimodal character. Several kinds of active species can thus be considered. In general, one high Mn population is present, which likely corresponds to slow initiation rate, possibly due to the heterogeneous character of the polymerization, as already observed previously with MOFs but also with classical Ziegler−Natta heterogeneous catalysts. This might be connected as well with neodymium compound, which is only partially active, and correlates well with the associated structure of the precatalyst (for one polymer chain per metal, without taking account of possible Nd−Al transfer[13]), as also considered with lanthanide carboxylate-based catalysts.[57] One may note that the bimodal character of macromolecular populations in terms of M_n can usually be seen as an advantage with respect to mechanical properties.[58] In contrast, when associated with MAO, precatalyst **4** (runs 5−8) affords polyisoprene, which displays quite monomodal SEC curves, although the PDI (polydispersity index, i.e., M_w/M_n) is rather broad. The molecular weights in the latter case (Mn_{exp}) are in the expected range (Mn_{th}) if one considers that all of the metal is involved in the polymerization process to produce polyisoprene (one polymer chain per Nd, Table 2). From this Mn_{exp}/Mn_{th} ratio, it is obvious in the case of the use of MMAO that all Nd compound is not activated to produce polyisoprene, as postulated above from the bimodal character of the SEC curves. Consequently, and as expected, crystalline residues with the typical related shape of the parent crystalline precatalyst can clearly be observed in the isolated material (see below).

Scanning Electron Microscopy (SEM) Macroscopic Examination. Compounds **3** and **4** have been analyzed by SEM by using the Hitachi S-3400N apparatus (Figure 4). After the hydrothermal treatment, as-synthesized crystallites of **3** with prismatic parallelepiped-like shapes of 20−120 μm size are observed. The phase **4** crystallized with specific needle shape of 200−1000 μm size. The SEM image (Figure 5) of the polyisoprene obtained with the as-synthesized precatalyst **3** clearly revealed some aggregates with 2−20 μm size randomly encapsulated at the surface of the polymer. The sizes of these blocks attributed to the residual solid **3** are smaller than those observed for the as-synthesized crystallites. A partial fragmentation of the precatalyst particles during the polymerization process could explain such a size difference as encountered in Ziegler−Natta heterogeneous catalysis.[59] The X-ray diffraction pattern still showed the signature of the crystalline precatalysts (Figure 6), which is heterogeneously mixed with the polyisoprene matrix. Similar observations are obtained with the precatalyst **4**, for which needle-shape crystallites with shorter lengths (30−100 μm) are visible at the surface of the polymer (Figure 5). For **3**, we also manually ground the as-synthesized crystallites in a mortar for 10 min. In this case, SEM image shows a smooth surface for the polymer, which is an indication of a better dissemination of the MOF in the polymer matrix. The X-ray diffraction patterns (Figure 6) of the polymeric material revealed some traces of the residual MOF phases. The observation of Bragg peaks shows that a part of the precatalysts is still crystalline, but the MOF content embedded within the polymer is quite low as indicated by the weak signal/noise ratio of the X-ray diffraction intensities.

Photoluminescence Properties. FT-Raman spectra were recorded to demonstrate the infrared (IR) photoluminescence capability of Nd(2,6-ndc)(form) (**3**) and $Nd(form)_3$ (**4**) materials (Figure 7); see the corresponding Experimental Section for details. To allow a comparison between the emission intensities of the two samples, all of the experimental setups were fixed (including grain size and packing of the samples); as a result, the two spectra have very similar base lines. The two compounds show the characteristic emission lines of the Nd^{3+} in the IR region, which are assigned to the $^4F_{3/2} \rightarrow {}^4I_{9/2}$, $^4F_{3/2} \rightarrow {}^4I_{11/2}$, and $^4F_{3/2} \rightarrow {}^4I_{13/2}$, intra $4f^3$ transitions between the first excited ($^4F_{3/2}$ state) and the Nd^{3+}ground multiplet levels ($^4I_{9/2}$, $^4I_{11/2}$, and $^4I_{13/2}$). Among them, the $^4F_{3/2} \rightarrow {}^4I_{11/2}$ transition, usually applicable to laser emission, is partially deleted due to the excitation cutoff filter but even though is expected to be dominant in both spectra. The distinct structure of the two compounds results in differentiable spectra, namely, by distinct emission intensities and Stark components distribution (Figure 7). Also, as expected, the vibronic transitions appearing in the Raman shift range 150−1200 cm^{-1} show a completely different profile (Figure 7). Unfortunately, no luminescence signal was detected for the Nd-based coordination polymers embedded into the polyisoprene material. This would be due to the very low concentration of the precatalyst present in the final polymer.

■ CONCLUSION

In this paper, we have described the synthesis and structural characterization of a series of neodymium-based MOFs, using the 2,6-naphthalenedicarboxylate or formate as organic linkers. The addition of other carboxylates such as oxalate or formate allows us to control the content of bonded water to the rare-earth center at the molecular level. Thanks to the absence of any aquo or hydroxo ligands bonded to the metal in the coordination polymer, the compounds were successfully used as precatalysts for the polymerization of isoprene. Combined with aluminoxanes, they afforded polymer in reasonable yield, up to 88.7% *cis*-regular.

dx.doi.org/10.1021/ic2019346 | *Inorg. Chem.* 2012, 51, 483−490

■ ASSOCIATED CONTENT

Supporting Information

CIF files for phases 1, 2, and 3. Infrared spectra, powder X-ray diffraction patterns, and X-ray thermodiffraction for phases 1, 3, and 4. This material is available free of charge via the Internet at http://pubs.acs.org.

■ AUTHOR INFORMATION

Corresponding Author

*E-mail: thierry.loiseau@ensc-lille.fr.

■ ACKNOWLEDGMENTS

We thank the Region Nord-Pas-De-Calais-Picardie for financial support (MULTI-NANO-MOF project) and T. Jarry & C. Renard (ISP Master Students) for their participation to this work, Nora Djelal, Laurence Burylo, and Catherine Meliet for their technical assistance. Prof. L. Carlos and J. Rocha (University of Aveiro, Portugal) are also acknowledged for measurement of the Nd luminescence spectra.

■ REFERENCES

(1) Yaghi, O. M.; O'Keeffe, M.; Ockwig, N. W.; Chae, H. K.; Eddaoudi, M.; Kim, J. *Nature* **2003**, *423*, 705.
(2) Kitagawa, S.; Kitaura, R.; Noro, S.-I. *Angew. Chem., Int. Ed.* **2004**, *43*, 2334.
(3) Férey, G. *Chem. Soc. Rev.* **2008**, *37*, 191.
(4) Janiak, C.; Vieth, J. K. *New J. Chem.* **2010**, *34*, 2366.
(5) Jiang, H.-L.; Xu, Q. *Chem. Commun.* **2011**, *47*, 3351.
(6) Zhao, D.; Timmons, D. J.; Yuan, D.; Zhou, H.-C. *Acc. Chem. Res.* **2011**, *44*, 123.
(7) Corma, A.; Garcia, H.; Llabres i Xamena, F. X. *Chem. Rev.* **2010**, *110*, 4606.
(8) Farrusseng, D.; Aguado, S.; Pinel, C. *Angew. Chem., Int. Ed.* **2009**, *48*, 7502.
(9) Isaeva, V. I.; Kustov, L. M. *Pet. Chem.* **2010**, *50*, 167.
(10) Lee, J. Y.; Farha, O. K.; Roberts, J.; Scheidt, K. A.; Nguyen, S. T.; Hupp, J. T. *Chem. Soc. Rev.* **2009**, *38*, 1450.
(11) Liu, Y.; Xuan, W.; Cui, Y. *Adv. Mater.* **2010**, *22*, 4112.
(12) Zhang, Z.; Cui, D.; Wang, B.; Liu, B.; Yang, Y. *Struct. Bonding (Berlin, Ger.)* **2010**, *137*, 49.
(13) Friebe, L.; Nuyken, O.; Obrecht, W. *Adv. Polym. Sci.* **2006**, *204*, 1.
(14) Visseaux, M.; Bonnet, F. *Coord. Chem. Rev.* **2011**, *255*, 374.
(15) Shen, Z. *Inorg. Chim. Acta* **1987**, *140*, 7.
(16) Fischbach, A.; Anwander, R. *Adv. Polym. Sci.* **2006**, *204*, 155.
(17) Vitorino, M. J.; Devic, T.; Tromp, M.; Férey, G.; Visseaux, M. *Macromol. Chem. Phys.* **2009**, *210*, 1923.
(18) Rosi, N. L.; Eddaoudi, M.; Kim, J.; O'Keeffe, M.; Yaghi, O. M. *CrystEngComm* **2002**, *4*, 401.
(19) Rosi, N. L.; Kim, J.; Eddaoudi, M.; Chen, B.; O'Keeffe, M.; Yaghi, O. M. *J. Am. Chem. Soc.* **2005**, *127*, 1504.
(20) Loiseau, T.; Mellot-Draznieks, C.; Muguerra, H.; Férey, G.; Haouas, M.; Taulelle, F. *C. R. Chim.* **2005**, *8*, 765.
(21) Senkovska, I.; Hoffmann, F.; Fröba, M.; Getzschmann, J.; Böhlmann, W.; Kaskel, S. *Microporous Mesoporous Mater.* **2009**, *122*, 93.
(22) Zhang, J.-Y.; Bu, J. T.; Chen, S.; Wu, T.; Zheng, S.; Chen, Y.; Nieto, R. A.; Feng, P.; Bu, X. *Angew. Chem., Int. Ed.* **2010**, *49*, 8876.
(23) Min, D.; Lee, S. W. *Bull. Korean Chem. Soc.* **2002**, *23*, 948.
(24) Almeida Paz, F. A.; Klinowski, J. *Chem. Commun.* **2003**, 1484.
(25) Zheng, X.; Sun, C.; Lu, S.; Liao, F.; Gao, S.; Jin, L. *Eur. J. Inorg. Chem.* **2004**, 3262.
(26) Almeida Paz, F. A.; Klinowski, J. *Acta Crystallogr. E* **2008**, *64*, m336.
(27) Almeida Paz, F. A.; Klinowski, J. *Acta Crystallogr. E* **2008**, *64*, m140.
(28) Deluzet, A.; Maudez, W.; Daiguebonne, C.; Guillou, O. *Cryst. Growth Des.* **2003**, *3*, 475.
(29) Wang, Z.; Jin, C.-M.; Shao, T.; Li, Y.-Z.; Zhang, K.-L.; Zhang, H.-T.; You, X.-Z. *Inorg. Chem. Commun.* **2002**, *5*, 642.
(30) Thomas, P.; Trombe, J. C. *J. Chem. Cryst.* **2000**, *30*, 633.
(31) Vaidhyanathan, R.; Narajan, S.; Rao, C. N. R. *J. Solid State Chem.* **2004**, *177*, 1444.
(32) Si, S.; Li, C.; Wang, R.; Li, Y. *J. Mol. Struct.* **2004**, *703*, 11.
(33) Dan, M.; Cottereau, G.; Rao, C. N. R. *Solid State Sci.* **2005**, *7*, 437.
(34) Xiao, F.; Lu, J.; Guo, Z.; Li, T.; Li, Y.; Cao, R. *Inorg. Chem. Commun.* **2008**, *11*, 105.
(35) Yang, Q.-F.; Yu, Y.; Song, T.-Y.; Yu, J.-H.; Zhang, X.; xu, J.-Q.; Wang, T.-G. *CrystEngComm* **2009**, *11*, 1642.
(36) Wang, Z.; Xing, Y.-H.; Wang, C.-G.; Sun, L.-X.; Zhang, J.; Ge, M.-F.; Niu, S.-Y. *CrystEngComm* **2010**, *12*, 762.
(37) Sun, Q.; Zhang, J.-Y.; Tian, H.; Wang, Y.-Q.; Gao, E.-Q. *Inorg. Chem. Commun.* **2009**, *12*, 426.
(38) Dai, F.; Cui, P.; Ye, F.; Sun, D. *Cryst. Growth Des.* **2010**, *10*, 1474.
(39) Deng, Z.-P.; Huo, L.-H.; Wang, H.-Y.; Gao, S.; Zhao, H. *CrystEngComm* **2010**, *12*, 1526.
(40) Han, Y.-F.; Zhou, X.-H.; Zheng, Y.-X.; Shen, Z.; Song, Y.; You, X.-Z. *CrystEngComm* **2008**, *10*, 1237.
(41) Deng, S.; Zhang, N.; Xiao, W.; Chen, C. *Z. Kristallogr. NCS* **2009**, *224*, 275.
(42) Lin, J.-M.; Guan, Y.-F.; Wang, D.-Y.; Dong, W.; Wang, X.-T.; Gao, S. *Dalton Trans.* **2008**, 6165.
(43) *SAINT Plus* Version 7.53a; Bruker Analytical X-ray Systems: Madison, WI, 2008.
(44) Sheldrick, G. M. *SADABS, Bruker-Siemens Area Detector Absorption and Other Correction*, Version 2008/1, 2008.
(45) Sheldrick, G. M. *Acta Crystallogr. A* **2008**, *64*, 112.
(46) Farrugia, L. J. *J. Appl. Crystallogr.* **1999**, *32*, 837.
(47) Terrier, M.; Visseaux, M.; Chenal, T.; Mortreux, A. *J. Polym. Sci., Part A: Polym. Chem.* **2007**, *45*, 2400.
(48) Lee, Y. K.; Lee, S. W. *Bull. Korean Chem. Soc.* **2003**, *24*, 948.
(49) Brese, N. E.; O'Keeffe, M. *Acta Crystallogr. B* **1991**, *47*, 192.
(50) Hirosaki, N.; Ogata, S.; Kocer, C. *J. Alloys Compd.* **2003**, *351*, 31.
(51) Mayer, I.; Steinberg, M.; Feigenblatt, F.; Glasner, A. *J. Phys. Chem.* **1962**, *66*, 1737.
(52) Pabst, A. *Can. Mineral.* **1978**, *16*, 437.
(53) Kistaiah, P.; Murthy, K. S.; Iyengar, L.; Rao, K. V. K. *J. Mater. Sci.* **1981**, *16*, 2321.
(54) Bolotovsky, R. L.; Bulkin, A. P.; Krutov, G. A.; Kudryashev, V. A.; Trunov, V. A.; Ul'yanov, V. A.; Antson, O.; Hiismäki, P.; Pöyry, H.; Tiita, A.; Loshmanov, A. A.; Furmanova, N. G. *Solid State Commun.* **1990**, *76*, 1045.
(55) Xu, Y.; Ding, S.-H.; Zhou, G.-P.; Liu, Y.-G. *Acta Crystallogr. E* **2006**, *62*, m1749.
(56) Go, Y.-B.; Jacobson, A. J. *Chem. Mater.* **2007**, *19*, 4702.
(57) Ferreira, L. C. Jr.; de Santa Maria, L. C.; Costa, M. A. S.; Tochetto Pires, N. M.; Nele, M.; Pinto, J. C. *Polym. Eng. Sci.* **2011**, *51*, 712.
(58) Bohm, L. L. *Angew. Chem., Int. Ed.* **2003**, *42*, 5010.
(59) Fink, G.; Steinmetz, B.; Zechlin, J.; Przybyla, C.; Tesche, B. *Chem. Rev.* **2000**, *100*, 1377.